

## Surface Modification of Electrospun Chitosan Nanofibrous Mats for Antibacterial Activity

Wiyong Kangwansupamonkon,<sup>1</sup> Walaiwan Tiewtrakoonwat,<sup>2</sup> Pitt Supaphol,<sup>3</sup>  
Suda Kiatkamjornwong<sup>2,4</sup>

<sup>1</sup>National Nanotechnology Center, National Science and Technology Development Agency, Klong Luang, Pathumthani 12120, Thailand

<sup>2</sup>Program of Petrochemistry and Polymer Science, Faculty of Science, Chulalongkorn University, Wangmai, Pathumwan, Bangkok 10330, Thailand

<sup>3</sup>The Petroleum and Petrochemical College and The Center of Excellence on Petrochemical and Materials Technology (PETROMAT), Chulalongkorn University, Wangmai Pathumwan, Bangkok 10330, Thailand

<sup>4</sup>Division of Science, The Royal Institute of Thailand, Sanam Sueba, Dusit, Bangkok 10300, Thailand

Correspondence to: S. Kiatkamjornwong (E-mail: ksuda@chula.ac.th)

**ABSTRACT:** Chitosan (CS) blended with poly(ethylene oxide) (PEO) was electrospun into nanofibrous mats. The spinning solution of 6.7 : 0.3 (% w/v) of CS : PEO was dissolved in a 70 : 30 (v/v) trifluoroacetic acid/dichloromethane solution. The obtained fibers were smooth without beads on their surfaces and average diameter of the fiber was  $272 \pm 56$  nm. *N*-(2-hydroxyl) propyl-3-trimethyl ammonium chitosan chloride (HTACC) and *N*-benzyl-*N,N*-dimethyl chitosan iodide (QBzCS) were each prepared from the CS/PEO mats. They were identified by Fourier-transform infrared and X-ray photoelectron spectroscopy and degree of swelling in water. Both quaternized electrospun chitosan mats exhibited superior antibacterial activity to the unmodified electrospun CS/PEO against *Staphylococcus aureus* and *Escherichia coli* at short contact times. After 4 h of contact, the reduction of both bacterial strains by CS/PEO, HTACC, and QBzCS was equal at about 99–100%. © 2014 Wiley Periodicals, Inc. *J. Appl. Polym. Sci.* **2014**, *131*, 40981.

**KEYWORDS:** antibacterial activity; biomaterials; electrospinning; fibers; grafting; nanostructured polymers

Received 27 December 2013; accepted 28 April 2014

DOI: 10.1002/app.40981

### INTRODUCTION

Chitosan (CS) is a polysaccharide which is typically produced by partial *N*-deacetylation of the natural polymer chitin. Chitin is a biopolymer present in the exoskeleton of crustaceans which can be obtained from shell waste of the crab, shrimp, and crawfish processing industries. Chitosan is a nontoxic copolymer consisting of  $\beta(1 \rightarrow 4)$ -linked 2-acetamido-2-deoxy- $\beta$ -*D*-glucopyranose and 2-amino-2-deoxy- $\beta$ -*D*-glucopyranose units. Chitosan is widely studied because of its excellent biological properties including wound healing and antibacterial properties.<sup>1,2</sup> The mechanism of the antimicrobial activity of CS and its derivatives is not clearly established. It has been suggested that chitosan derivatives with quaternary ammonium groups possess high efficacy against bacteria and fungi. It is now widely accepted that the target site of these cationic polymers is the negatively charged cytoplasmic membranes that lead to leakages of intracellular constituents.<sup>3–8</sup> Electrospinning is an interesting technique for fabricating continuous polymer fibers from solu-

tions or melts with average diameters in sub-micrometer down to nanometer range using the action of an external electric field. The morphology and diameters of electrospun fibers depend on a number of parameters, that include properties and composition of the spinning solution such as polymer type, conformation of polymer chain, viscosity or concentration of the solution, conductivity, polarity and surface tension of the solvent, and processing conditions, such as applied field strength, distance between the capillary and collector, and feeding rate.<sup>9–12</sup> These fibers produced by electrospinning exhibit several amazing characteristics such as a very large surface area-to-mass or volume ratio and a small inter-fibrous pore size with high porosity, vast possibilities for surface functionalization, and many others.<sup>10,11,13,14</sup>

This work reports the successful preparation of electrospun nanofibrous mats from the chitosan solutions in a trifluoroacetic acid (TFA) and dichloromethane (DCM) co-solvent system<sup>15</sup> and PEO is used as the non-ionogenic partner: all of

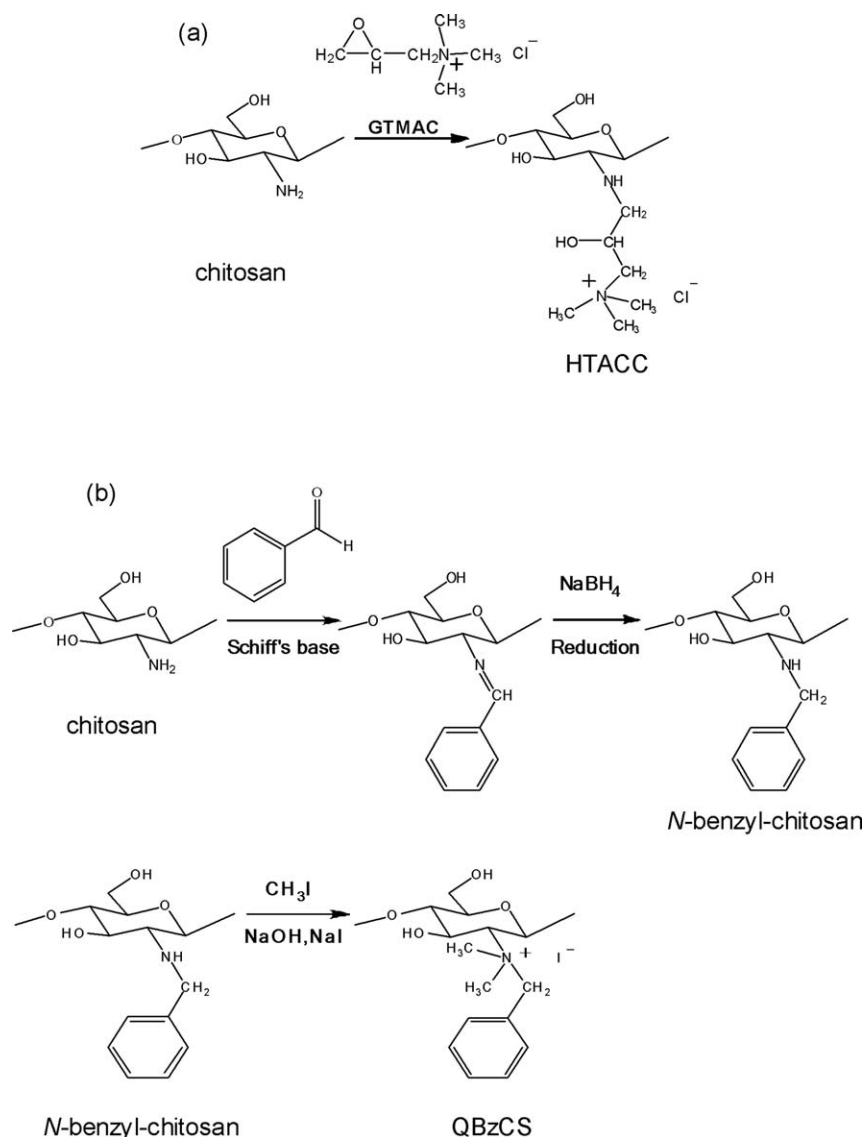


**Figure 1.** Surface modification of chitosan with (a) GTMAC, and (b) *N*-benzyl-*N,N*-dimethyl-chitosan iodide (QBzCS).

which facilitate the electrospinning. Modification of the surface amino groups with glycidyl trimethyl ammonium chloride (GTMAC), or benzaldehyde/methyl iodide was conducted to give *N*-[(2-hydroxyl-3-trimethyl ammonium) propyl] chitosan chloride (HTACC) in Figure 1(a) and *N*-benzyl-*N,N*-dimethyl chitosan iodide (QBzCS) in Figure 1(b), respectively, and both are considered to be a potent antibacterial agent.

The antibacterial activity of the surface modified HTACC and QBzCS nanofibrous mats against the Gram-positive bacteria *Staphylococcus aureus* and Gram-negative bacteria *Escherichia coli* are assessed and compared with the unmodified CS/PEO electrospun mat. All the modified mats could inhibit *S. aureus* growth better than the unmodified mat and this inhibition of *S. aureus* was greater than that for *E. coli*. The antibacterial efficiency was greater after 1 and 2 h bacterial contact with the spun mats than 0.5 h, and an equal antibacterial efficiency was achieved with the longer contact time.

## EXPERIMENTAL

### Materials

Chitosan (CS) powder (degree of deacetylation of 84%), trifluoroacetic acid (TFA, C<sub>2</sub>HF<sub>3</sub>O<sub>2</sub>, 98% purity), and glycidyl trimethyl ammonium chloride (GTMAC, C<sub>6</sub>H<sub>14</sub>ClNO, analytical grade) were purchased from Fluka (Germany). Poly(ethylene oxide) (PEO) with an average molecular weight of 600 kDa, sodium borohydride (NaBH<sub>4</sub>), methyl iodide (CH<sub>3</sub>I), and glutaraldehyde (C<sub>5</sub>H<sub>8</sub>O<sub>2</sub>, 25% in H<sub>2</sub>O) were purchased from Sigma-Aldrich. Benzaldehyde (C<sub>7</sub>H<sub>6</sub>O) was purchased from Acros Organic. Sodium carbonate (Na<sub>2</sub>CO<sub>3</sub>) was purchased from Ajax Finechem (New Zealand). Acetic acid (C<sub>2</sub>H<sub>4</sub>O<sub>2</sub>), methanol (C<sub>2</sub>H<sub>4</sub>O), ethanol (C<sub>2</sub>H<sub>6</sub>O), dichloromethane (DCM, C<sub>2</sub>H<sub>2</sub>Cl<sub>2</sub>), and sodium hydroxide (NaOH) were purchased from Lab-Scan Analytical Science (Ireland). All other reagents were analytical grade and used without further purification. *E. coli* ATCC 25922 and *S. aureus* ATCC 6538 used as models for

Gram-negative bacteria and Gram-positive bacteria, respectively, were obtained from the Department of Medical Science (Ministry of Public Health, Thailand). For the growth culture, single colonies of bacteria were inoculated in Tryptic Soy Broth (TSB) and incubated aerobically at 37°C for 24 h.

### Spinning Solution and Fabrication of Electrospun CS Fibrous Mats

A spinning solution of 7% (w/v) CS/PEO solution was prepared by dissolving specific amounts of CS and PEO at various weight ratios in a co-solvent system of TFA and DCM at a volumetric ratio of 70 : 30. Each solution was stirred for 18 h before subjecting to an electrospinning process.

Chitosan fibrous mats were prepared by electrospinning the CS/PEO solution at  $25 \pm 1^\circ\text{C}$  and the relative humidity of  $70 \pm 2\%$ . Electrospinning of the as-prepared solutions was performed by connecting the emitting electrode of positive polarity from a Gamma High-Voltage Research ES30PN/M692 high-voltage DC power supply to the solutions contained in a standard 50-mL syringe, the open end of which was attached to a blunt gauge-20 stainless steel needle having an outer diameter of 0.91 mm, used as the nozzle, and the grounding electrode to a home-made rotating metal drum having an outer diameter of 9 cm used as a fiber collector. A fixed electrical potential of 20 kV was applied across a fixed distance of 20 cm between the tip of the nozzle and the outer surface of the drum when the rotational speed of the rotating drum was  $60 \pm 5$  rpm. For the first set of CS/PEO mats, the obtained fibrous mats were dried *in vacuo* at 25°C for 24 h prior to being crosslinked with glutaraldehyde vapor in a desiccator for 6 h at 25°C. After the crosslinking, the mats were then dried in vacuum for 24 h. For the second set of the mats, the crosslinked mats were neutralized further in 5M Na<sub>2</sub>CO<sub>3</sub> aqueous solution for 3 h to reduce swelling extent of electrospun mat, washed afterwards several times with deionized (DI) water, and finally dried at 25°C for 24 h.<sup>16</sup>

### Surface Modification of Electrospun CS Fibrous Mats by GTMAC

HTACC fibrous mats were synthesized according to the established method as outlined in Figure 1(a).<sup>17</sup> Four pieces of crosslinked CS/PEO fiber mats ( $6 \times 3$  cm<sup>2</sup>) weighing about 0.5 g or the crosslinked/neutralized mats were placed into a reaction vessel filled with 40 mL of DI water containing a specific amount of GTMAC at the CS-to-GTMAC mole ratio at 1 : 4. The reaction was performed at 70°C and gently stirred with a magnetic stirrer for 12 h. The modified CS/PEO fibrous mats were washed with DI water, and ethanol was later added to remove the unreacted GTMAC. The mats were dried *in vacuo* at 25°C for 1 day.

### Surface Modification of Electrospun CS Fibrous Mats by N-Benzyl-N,N-Dimethyl Ammonium Iodide

Surface quaternized chitosan derivative (QCS) namely N-benzyl-N,N-dimethyl chitosan iodide (QBzCS), as shown in Figure 1(b), was prepared by a modified method according to the two-step procedure described elsewhere.<sup>18–20</sup> The CS/PEO mats were neutralized in 5M Na<sub>2</sub>CO<sub>3</sub> aqueous solution for 3 h, washed several times with deionized water and dried at 25°C for 24 h.<sup>16</sup> In the first step of modification, each of the neutralized CS/

PEO mats cut in a circular form having a diameter of 1.4 cm and weighing about 40 mg was immersed in 4.3 mL of 5% (v/v), (0.0021 mol) of benzaldehyde solution in anhydrous methanol for 12 h at 50°C. After stirring for a given time, NaBH<sub>4</sub> (120 mg, 0.0032 mol, i.e., 1.5 time of benzaldehyde concentration) was added into the reaction mixture and the solution was stirred for 24 h at 50°C. The mats were removed from the solution, rinsed thoroughly with methanol, and dried *in vacuo*. In the next step, an anhydrous methanol solution of NaI (0.2M) and NaOH (0.4M) was added into a flask containing N-alkyl chitosan mat having a diameter of 1.4 cm (40 mg) and then CH<sub>3</sub>I (1.6M) was added in the mixed solution. The reaction mixture was stirred at 50°C for an indicated time (6, 12, 18, and 24 h). Then, the mats were removed from the solution, rinsed thoroughly with methanol, and dried *in vacuo*.

### Characterization

Morphologies of the unmodified and the modified CS/PEO fibrous mats were investigated by scanning electron microscopy (SEM, JEOL JSM-5200, Japan). The fiber mats were coated with gold (JEOL JFC-1100E sputtering device, Japan) for 3 min prior to the SEM observation.

Fourier-transform infrared spectroscopy (FTIR, Nicolet Nexus 671, U.K.) and the degree of swelling were used to confirm the success of the modification reaction. The degree of swelling was determined gravimetrically. Each specimen, after being submerged in DI water for 1 h, was sandwiched between a pair of paper towels. A flat metal sheet (500 g) was placed on top of each specimen to remove excessive amount of water. The degree of swelling (S) was then calculated according to eq. (1):

$$S(\%) = \frac{W_2 - W_1}{W_1} \times 100, \quad (1)$$

where  $W_1$  and  $W_2$  are weights of the specimen in its dried and swollen state, respectively.

A Tetra Probe X-ray photoelectron spectroscopy (Thermo Fisher Scientific, U.K.) was used to investigate binding energy of the elements on the surface of the fibrous mats with MoK<sub>α</sub> source for excitation at 10 mA and 20 kV. Detailed spectra were recorded for the region of C 1s and N 1s with a 0.1 eV interval. The C 1s line at 285.0 eV was used for an energy calibration. The XPS spectra were collected at room temperature. The degree of quaternization, %DQ, was then calculated according to eq. (2):

$$\%DQ = \frac{\%N^+R_1R_2R_3}{\%NH_2 + \%N^+R_1R_2R_3}, \quad (2)$$

when  $R_1$ ,  $R_2$ , and  $R_3$  are the methyl groups ( $-\text{CH}_3$ ) for the case of HTACC/PEO and  $R_1$  is the benzyl group ( $-\text{Bz}$ ), and  $R_2$  and  $R_3$  are the methyl groups ( $-\text{CH}_3$ ) for the case of QBzCS/PEO.

### Antibacterial Activity Assessment

The antibacterial activity of the unmodified CS/PEO and the modified HTACC and QBzCS electrospun mats against the Gram-positive bacteria *S. aureus* ATCC No. 6538 and Gram-negative *E. coli* ATCC No. 25922 was assessed by a viable cell-counting method. Each of the electrospun mats (30 mg),

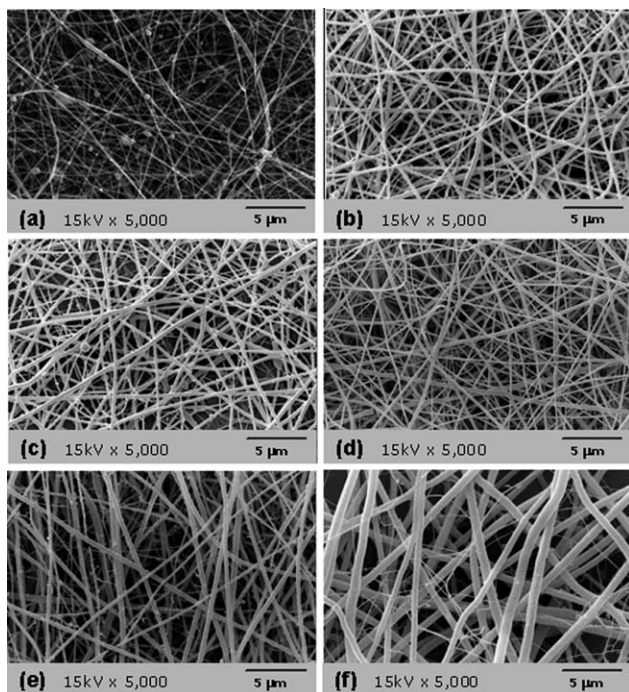


**Figure 2.** SEM images of CS/PEO fiber obtained from different CS : PEO weight ratios to give various fiber diameters: (a) 7 : 0 with  $148 \pm 42$  nm, (b) 6.9 : 0.1 with  $234 \pm 49$  nm, (c) 6.8 : 0.2 with  $265 \pm 47$  nm, (d) 6.7 : 0.3 with  $271 \pm 56$  nm, (e) 6.6 : 0.4 with  $350 \pm 84$  nm, and (f) 6.5 : 0.5 with  $624 \pm 107$  nm.

sterilized by 254-nm wavelength UV irradiation for 15 min, was added into a suspension of the bacteria containing TSB ( $6 \text{ cm}^3$  containing about  $1\text{--}5 \times 10^5$  colony-forming unit per mL, CFU  $\text{cm}^{-3}$ ) and then the suspension was stirred and incubated in a volumetric flask at  $37^\circ\text{C}$ . At a specified time of incubation,  $1 \text{ cm}^3$  of each bacteria culture was added to  $9 \text{ cm}^3$  of sterilized 0.9% phosphate buffer saline solution at a pH about 7.4. This pH (7.4) at the isotonic condition is used mainly for bacterial survival purposes during dilution stage and cell counting stage because an equal concentration of the solution exists inside and outside the cell and the solutions match the osmotic pressure of the human blood. The surviving bacteria were transferred onto a separate Trypticase Soy Agar (TSA) plate using an Automated Spiral Plating System (Autoplate 4000, Spiral Biotech, Norwood, MA) and then the plate was incubated at  $37^\circ\text{C}$ . After incubation for 24 h, the colonies were counted using an automatic colony counter (Flash & Go, IUL Instruments, Spain). Triplicate counting was done for each experiment. The reduction of bacteria was calculated according to eq. (3):

$$\text{Reduction (\%)} = \frac{(A-B)}{A} \times 100, \quad (3)$$

where  $A$  and  $B$  are the surviving cells (CFU  $\text{cm}^{-3}$ ) for the plates containing the control and test samples, respectively, after 0.5, 1.0, 2.0, 4.0, and 24 h contact time.

#### SEM Examination on the Bacterial Cells

SEM was used as a tool to directly observe the morphological changes of the tested bacterial strains before and after the cells were in contact with the electrospun mats. Bacteria cells

( $10^5$  CFU  $\text{cm}^{-3}$ ) were dropped onto a  $1 \times 1 \text{ cm}^2$  electrospun mat and incubated at  $37^\circ\text{C}$  for 24 h. The electrospun mats were washed with phosphate buffered saline (PBS) for one to two times and fixed with 3% glutaraldehyde at  $4^\circ\text{C}$  for 24 h. After the cell fixation, a dehydration process was conducted for 10 min in each concentration with 1 mL of 30, 50, 70, 90, and 100% ethanol. The fixed cell was dried and gold-coated using an ion sputter (JEOL JFC-1100E sputtering device, Japan). The pre-treated samples were observed by SEM (JEOL JSM-5200, Japan).

## RESULTS AND DISCUSSION

### Fabrication of Electrospun Chitosan Fibrous Mats

Representative SEM images of the obtained fibrous mats are shown in Figure 2. The diameters of the neat CS fibrous mats varied rather widely, with the presence of beaded segments as well as discrete beads distributing throughout the spun mat [Figure 2(a)]. PEO was thus selected as a suitable non-ionic template for the preparation of the smooth electrospun chitosan fibers.<sup>21</sup> Inevitably, the morphologies of the obtained CS/PEO fibers were strongly influenced by the weight ratio of the two polymers in the spinning solutions. At the CS : PEO ratio of 6.9 : 0.1 (w/w), the polymer solution could not be ejected from the nozzle of the needle as a continuous jet stream and some discrete drops of the solution were occasionally observed on the collection screen, despite the rather smooth fiber surface being observed in the SEM image [Figure 2(b)]. The electrospinnability of the solution was improved greatly at the CS : PEO ratio of 6.8 : 0.2 (w/w) [Figure 2(c)]. However, the beads disappeared completely at the CS : PEO ratio of 6.7 : 0.3 (w/w) [Figure 2(d)]. Further increases in the PEO content in the solutions to 0.4 [Figure 2(e)] and 0.5% (w/v) [Figure 2(f)] helped facilitate the electrospinning to a greater extent. Analyses of the diametric distribution of the obtained fibers reveal a marked increase in the fiber diameters from  $148 \pm 41$  nm of the neat CS fibers to  $234 \pm 41$  nm of the 6.9 : 0.1 (w/w) CS/PEO fibers and finally to  $624 \pm 106$  nm of the 6.5 : 0.5 (w/w) CS/PEO fibers.

### Surface Modification of Electrospun CS Fibrous Mats by Glycidyl Trimethyl Ammonium Chloride

The 6.7 : 0.3 (w/w) CS/PEO fiber mats were chosen for the crosslinking reaction because of its stability in neutral and basic condition, its ease in spinning and fine nanofibrous structure without discrete beads or beaded fibers being observed. The fiber mats were thus crosslinked with glutaraldehyde (GT) vapor to limit the dissolution of the CS-TFA salts<sup>15,16</sup> and the PEO. When the CS/PEO fiber mats were cross-linked with GT vapor, the mats retained their fibrous structure during the HTACC modification. In addition, the disappearance of the IR transmittance peak at  $1587 \text{ cm}^{-1}$  (Figure 3) of the crosslinked CS/PEO fiber mat indicated that the free amino groups were modified.<sup>21</sup>

Seong et al.<sup>17</sup> elucidated that HTACC was synthesized from the reaction between GTMAC and the amino groups of CS as shown in Figure 1(a). Under the acidic condition, GTMAC reacted mainly with the amino groups; while under the alkaline condition, GTMAC reacted similarly with the hydroxyl groups.

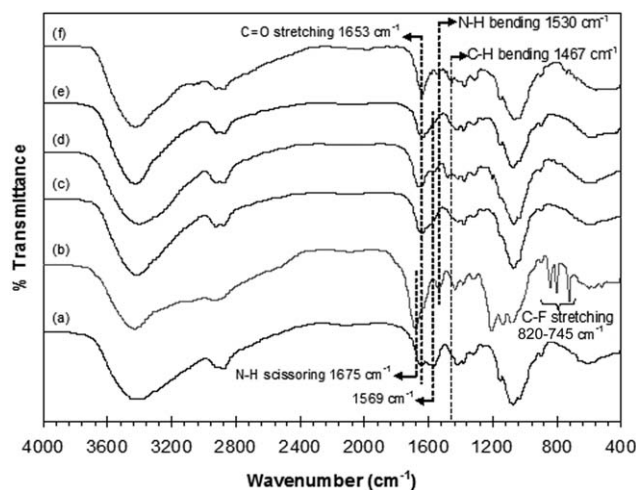


**Figure 3.** FTIR spectra of (a) chitosan, (b) CS/PEO fibrous mat, (c) crosslinked CS/PEO, (d) crosslinked HTACC, (e) crosslinked/neutralized CS/PEO, and (f) crosslinked QBzCS fibrous mats.

Figure 3 shows the FTIR spectra of the neat CS, CS/PEO fibrous mats, crosslinked CS/PEO fibrous mats, HTACC fibrous mat, neutralized CS/PEO fibrous mat, and QBZCS fibrous mat. Characteristic peaks of the neat CS [Figure 3(a)] at  $3400\text{ cm}^{-1}$  are for  $\text{—OH}$  and  $\text{—NH}_2$  stretching;  $1653$  and  $1569\text{ cm}^{-1}$  for  $\text{—NH}_2$  scissoring and bending, respectively. The characteristic transmittance peaks of the chitosan fiber were observed at  $1675$  and  $1530\text{ cm}^{-1}$ , corresponding to the stretching of the proto-

nated amino ( $\text{—NH}_3^+$ ) groups. The large peak at around  $1675\text{ cm}^{-1}$  and three absorption peaks around  $845\text{—}720\text{ cm}^{-1}$  [Figure 3(b)] indicated the presence of TFA in CS/PEO fibers as amine salts.<sup>15,16,22</sup>

The CS/PEO mat was crosslinked by GT before the modification because the mat could dissolve in aqueous solution of GTMAC caused by the ionic interaction between the amino group and TFA to become the ammonium salt. The CS/PEO mat changed to yellowish color after the crosslinking reaction. Figure 3(c) shows a new peak of imine functionality at  $1653\text{ cm}^{-1}$  due to the interaction between the amino group in CS and the aldehyde group of GT. Although the peaks of amino group at  $1675$  and  $1530\text{ cm}^{-1}$  disappeared. Schiffman and Schauer<sup>24</sup> postulated that the imine peak observed at  $1620\text{—}1660\text{ cm}^{-1}$  and could also overlap with the amino group of CS. In the FTIR spectra of HTACC fibrous mats [Figure 3(d)], the amino peak at  $1530\text{ cm}^{-1}$  disappeared and a new peak at  $1487\text{ cm}^{-1}$  evolved for the methyl stretching from  $\text{—N(CH}_3\text{)}$  of CS indicating that the epoxide ring of GTMAC had coupled with the  $\text{—NH}_2$  groups of CS [Figure 1(a)]. Figure 3(e) shows that the neutralized first and then crosslinked CS/PEO mat did not exhibit the peak at  $1487\text{ cm}^{-1}$  of the methyl groups which indicated that GTMAC did not interact with the amino group of the CS/PEO mat. This observation could be confirmed by degree of water swelling of the mats.<sup>23</sup> Actually, the non-neutralized CS/PEO absorbed a greater amount of water ( $758 \pm 66\%$ ) whereas the neutralized counterpart absorbed just  $134 \pm 7\%$  because CS/PEO has the higher hydrophilicity due to

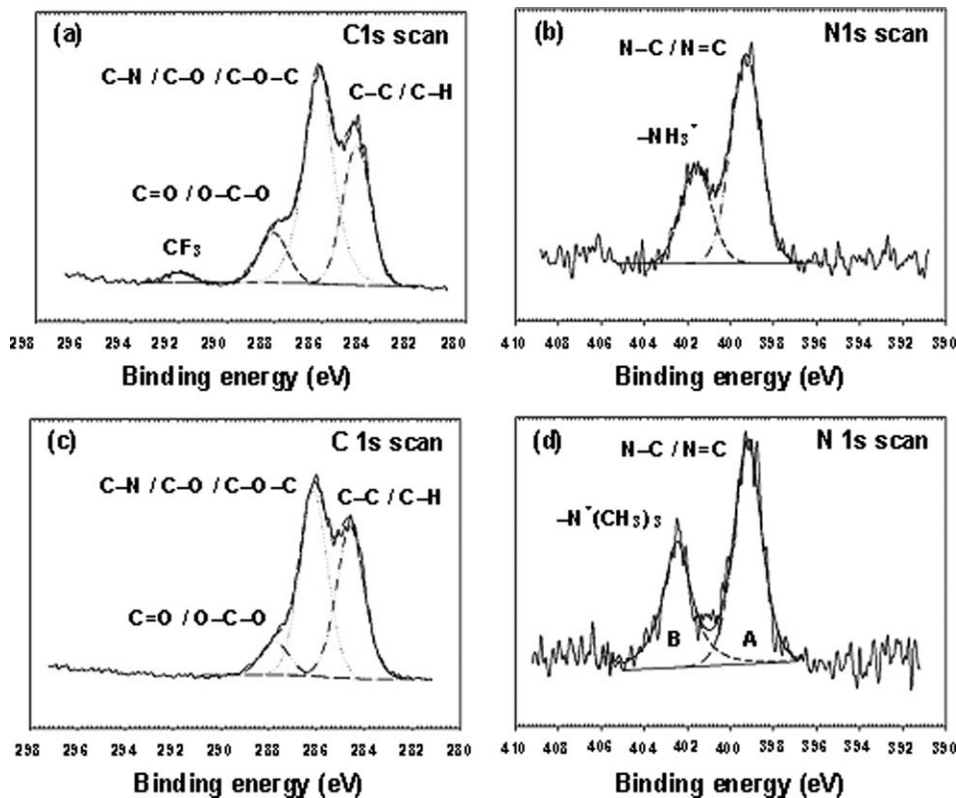


**Figure 4.** XPS spectra of (a) C 1s scan of crosslinked CS/PEO, (b) N 1s scan of crosslinked CS/PEO, (c) C 1s scan of HTACC, and (d) N 1s scan of HTACC having the peak area A and B = 3.5 and 1.8, respectively, to give 40.7% grafting.

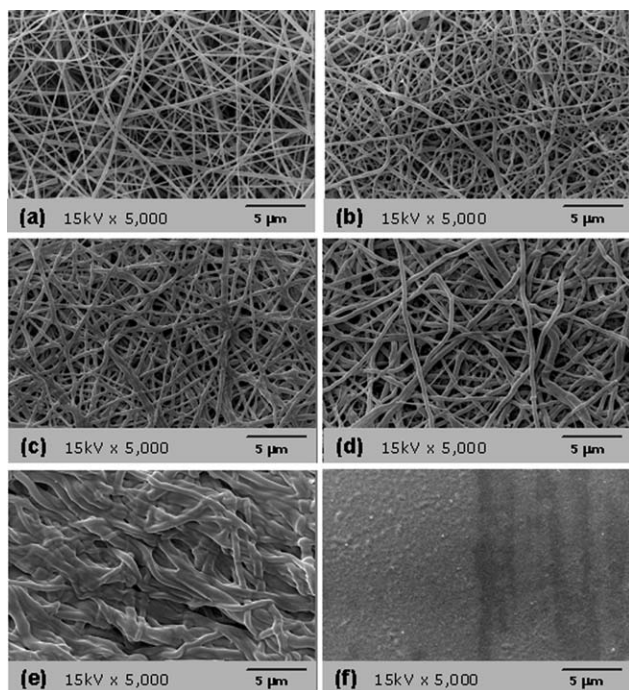


**Figure 5.** SEM images of (a) CS/PEO fiber, (b) neutralized CS/PEO fiber, and (c–f) QBzCS at different reaction times of methylation at 6, 12, 18, and 24 h.

the protonated ammonium salt. Degree of swelling of the HTACC from the reaction of GTMAC with the neutralized CS/PEO fibrous mats was almost constant at a range from  $146 \pm 4\%$  to  $153 \pm 23\%$  from 2-h to 24-h grafting time whereas those from the non-neutralized fiber mats ranged from  $154 \pm 12$  to  $306 \pm 19\%$  when increasing the same reaction time. When increasing the reaction time, hydrophilicity of the HTACC fibrous mats gradually increased. The surface of HTACC fibrous mats still needs more modification and improvement in packing ability of chitosan, that is, intermolecular hydrogen interaction between CS molecules improved the molecular packing after the neutralization as evidenced by the two XRD peaks of the neutralized mat at  $10.2$  and  $20.3^\circ$ , the crystalline regions of chitosan.<sup>16</sup> In the reaction of GTMAC with the non-neutralized CS/PEO fibrous mats, protonated ammonium groups reacted with the epoxide ring of GTMAC and decreased the hydrophilicity of the mats.

The results of XPS spectral study for the crosslinked CS/PEO fibrous mat and HTACC fibrous mat are shown in Figure 4. The C1s spectrum of the crosslinked CS/PEO fibrous mats had three components [Figure 4(a)] at 284.6 eV, 286.3 eV, and 288.0 eV with a relative intensity ratio of 1 : 1.3 : 0.3, attributed to C–C (or C–H), C–N (or C–O or C–O–C), and C=O (or O–C–O) carbons, respectively.<sup>25</sup> The clearly visible carbon peak (–CF<sub>3</sub>) of TFA at 292.2 eV disappeared completely, suggesting that the TFA was completely removed from HTACC fibrous mats [Figure 4(c)]. The N1s peak in the spectrum of the crosslinked CS/PEO fibrous mats, located at 399.3 eV and 401.7 eV [Figure 4(b)], is attributed to N–C (or N=C) and quaternary ammonium (–NH<sub>3</sub><sup>+</sup>) due to the protonated amino nitro-

gen by TFA, respectively. For HTACC fibrous mat, the N1s peak located at 339.2 eV and 402.5 eV is attributed to N–C (or N=C) and quaternary ammonium (–N<sup>+</sup>(CH<sub>3</sub>)<sub>3</sub>) from the grafting process. The %DQ in the surface region estimated from the eq. (2) using the relative ratio of atomic composition of peak A to peak B from Figure 4(d). For the HTACC fibrous mats, it was found that the %DQ of the HTACC fibrous mats after the quaternization was 40.7%.

#### Surface Modification of Electrospun CS Fibrous Mats by *N*-Benzyl-*N,N*-Dimethyl Ammonium Iodide

The *N*-benzyl-*N,N*-dimethyl-chitosan iodide was prepared from the neutralized 6.7 : 0.3 (w/w) CS/PEO fibrous mats by alkylation and methylation reactions. After methylation reaction at 6, 12, 18, and 24 h intervals, the morphologies of fibrous mats changed. The SEM image of CS/PEO fibrous mat before neutralization is shown in Figure 5(a), after being neutralized with Na<sub>2</sub>CO<sub>3</sub>, the stabilized fibrous mat was obtained as shown in Figure 5(b). The CS/PEO fibrous mat can swell and dissolve in water because the remaining TFA protonates the amino groups of CS to form the ammonium salts which is water soluble. Therefore, the neutralization between CS/PEO fibrous mat and Na<sub>2</sub>CO<sub>3</sub> can regenerate the amino groups which make the neutralized CS/PEO more stable. After 6 and 12 h of methylation, the modified fibrous mat [Figure 5(c,d)] could maintain the fiber shape. Unfortunately, after 18 h of methylation, the modified fibrous mat [Figure 5(e)] fused together; and after 24 h of methylation, the QBzCS could dissolve in anhydrous methanol and a film [Figure 5(f)] was formed without the presence of any fiber-like structure. Although more hydrophobicity was introduced to CS/PEO chains the quaternized nitrogen chains with the positive charge coupled with its anionic counter part of iodide facilitate hydrophilicity of the final QBzCS fibrous mats.

The FTIR spectrum of QBzCS fibrous mat was similar to that of neutralized CS/PEO as shown in Figure 3(e). The QBzCS fibrous mat exhibited the characteristic IR peaks at  $1530 \text{ cm}^{-1}$  and  $1467 \text{ cm}^{-1}$  attributed to the N–H bending and C–H bending of the methyl substituent of quaternary ammonium groups [Figure 3(f)], respectively. Thus, the XPS analysis further supports the success of surface quaternization on CS/PEO fibrous mats (Figure 6).

Besides C, O, and N which are the basic elements already present in the neutralized CS/PEO fibrous mat, no additional elements introduced to the chitosan fibrous mat surface after the reductive *N*-alkylation and methylation reactions were found in Figure 6(a,b). The only way to detect the quaternary ammonium groups after the surface modification is to consider the N1s spectrum and I3d<sub>5</sub> spectrum of the surface quaternized chitosan fibrous mat in comparison with the neutralized CS/PEO fibrous mat. As seen from Figure 6(a), the N1s peak of the neutralized CS/PEO fibrous mat can be fitted with one peak at 399.4 eV and no peak appears in I3d<sub>5</sub> spectrum. The N1s signals of QBzCS fibrous mats [Figure 6(c)], conversely, can be split into two peaks. The first one appears at the same binding energy as the CS/PEO fibrous mat (peak A). The second one having a higher binding energy emerges at 402 eV (peak B).

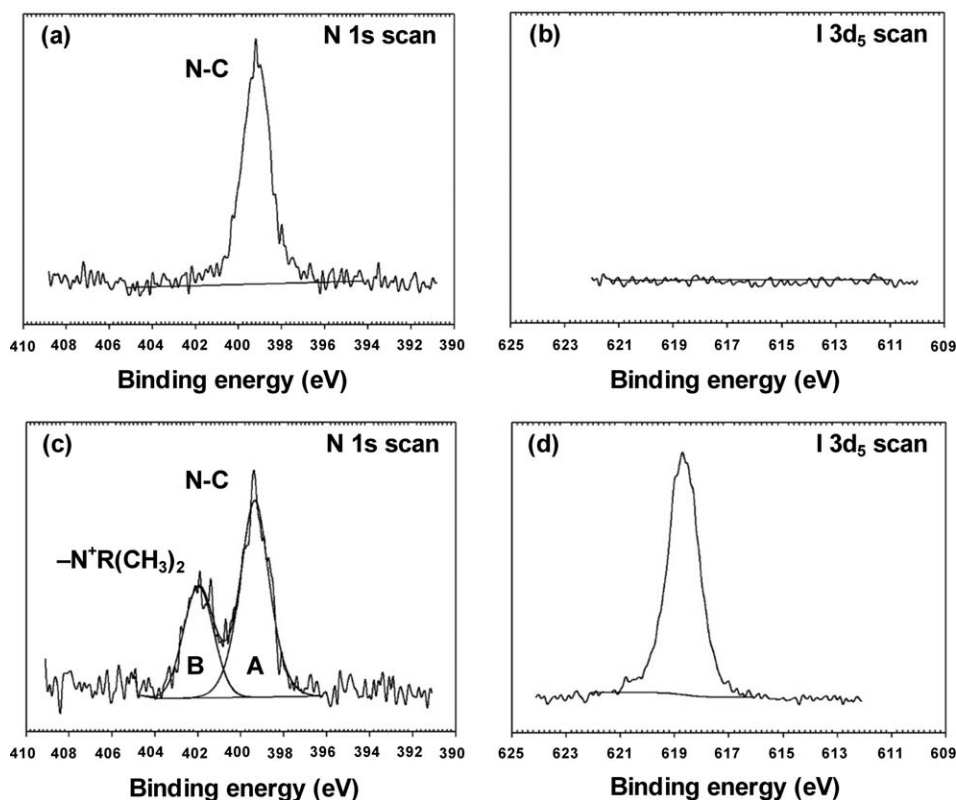


**Figure 6.** XPS spectra of (a) N 1s scan of neutralized crosslinked CS/PEO (b) I 3d<sub>5</sub> scan of neutralized CS/PEO (c) N 1s scan of QBzCS to having A and B = 2.2 and 3.9 giving a grafting of 36.1% and (d) I 3d<sub>5</sub> scan of QBzCS.

This latter peak can be regarded as a signal from the positively charged nitrogen atom of the quaternary ammonium moiety. The I3d<sub>5</sub> peak of the QBzCS fibrous mat can be fitted with the single peak at 618.7 eV of the counter ion [Figure 6(d)]. The atomic composition of peak A-to-peak B ratio from Figure 6(c) can be used for estimating the %DQ in the surface region from eq. (2). For the QBzCS fibrous mats, it was found that the %DQ of the *N*-benzyl chitosan fibrous mat after the quaternization with 0.4M NaOH and 1.6M CH<sub>3</sub>I was 36.1%.

#### Antibacterial Activities Assessment

Considering surface properties of the three materials, Vallapa et al.<sup>19</sup> reported that the water contact angle of QBzCS was  $93.3 \pm 2.3^\circ$  because QBzCS is relatively hydrophobic due to the *N*-benzyl end group. The HTACC surfaces are more polar than the CS/PEO. The polarity of both the HTACC and CS/PEO surfaces is, of course, higher than of the QBzCS. Based on the surface properties of the antibacterial nanofibrous mats that can interact with the bacterial cell wall, the initial contact and the lead time for the antibacterial mats to do adsorption on the cell wall is of prime importance for the antibacterial activity. The extent of antibacterial activity reported as %bacterial reduction caused by the two surface-modified and one un-modified electrospun chitosan mats examined against the Gram-positive and Gram-negative bacteria, *S. aureus* and *E. coli*, respectively, as a function of contact time is presented in Table I.

**Gram-Positive *S. aureus*.** As shown in Table I, *S. aureus* contacted with the three electrospun chitosan mats at the contact

times of 0.5, 1, and 2 h, the antibacterial activities of *S. aureus* can be ranked in the decreasing order as follows: QBzCS > HTACC > CS/PEO. When the bacterial contact times were longer than 2 h until 24 h, all the three fibrous mats gave the same antibacterial activity at 99%. It implied that reduction of the bacteria increased with contact time but with much higher reduction at the short contact time, that is, its bacterial reduction ability increased rapidly (about 40%) with the short contact time at 0.5-h contact time to become 99.95% at 24-h contact time. On the other words, the efficiency of bacterial reduction at the shorter contact is more pronounced than those of the longer contact times. It was anticipated that antibacterial efficiencies at the earlier stage of contact are much more beneficial for medical care.

**Gram-Negative *E. coli*.** The antibacterial activities of CS/PEO and HTACC contacted with *E. coli* at 0.5 h were 8.1 and 8.4%, respectively, which indicated that the activities of these two mats were not much different at the short contact time. However, QBzCS fibrous mat could produce a much higher antibacterial activity at 30.5% and up to 82.6% at 0.5 h and 2 h of contact time, respectively. Beyond 2 h till 24 h, all three antibacterial mats gave the same maximum reduction in bacterial activity (99–100%).

As a general observation, more antibacterial effectiveness was observed on both surface modified chitosan mats during the short contact time which is very important for medical

**Table I.** Reductions of *S. aureus* and *E. coli* When Contact with CS/PEO, HTACC, and QBzCS Fibrous Mats at Various Times

Type of bacteria	Contact time (h)	% Reduction <sup>a</sup>		
		CS/PEO	HTACC <sup>b</sup>	QBzCS <sup>c</sup>
Gram positive <i>S. aureus</i>	0.5	6.9 ± 2.3	25 ± 8.4	40.0 ± 11.2
	1	8.0 ± 3.9	33.1 ± 5.4	50.5 ± 3.7
	2	72.4 ± 13.5	73.3 ± 10.1	72.3 ± 0.4
	4	99.3 ± 0.2	99.7 ± 0.5	99.3 ± 0.0
	24	99.9 ± 0.0	99.9 ± 0.0	99.9 ± 0.0
Gram negative <i>E. coli</i>	0.5	8.1 ± 2.9	8.5 ± 4.9	30.5 ± 6.2
	1	8.7 ± 4.9	19.8 ± 3.6	39.3 ± 9.3
	2	71.6 ± 7.2	79.7 ± 3.0	82.6 ± 1.5
	4	98.5 ± 1.1	98.6 ± 1.6	98.5 ± 0.2
	24	100 ± 0.0	100 ± 0.0	100 ± 0.0

<sup>a</sup>The number of replication is three.

<sup>b</sup>40.7% grafting.

<sup>c</sup>36.1% grafting.

application because more than sixfold of bacteria were killed by QBzCS fibrous mat.

The HTACC fibrous mat could reduce the *S. aureus* activity more superior to that of CS/PEO. But for the *E. coli* bacteria, QBzCS could do the better reduction in bacterial activities. This can be explained that the complex cell wall of *E. coli* prevented the mats to attack their wall. Besides the relative hydrophobicity of the QBzCS antibacterial mat, the benzyl end group attached with dimethylated moiety of QBzCS contributed to the superior antibacterial activity than those of the trimethylated one (HTACC) and the protonated amino group of CS because the latter two mats (CS/PEO and HTACC) are more hydrophilic in nature. The quaternary moiety which is attached with the methylene group, giving a longer spacer to the CS backbone, produced the better antibacterial activity than did the positive charge of protonated CS. In the three antibacterial mats, CS/PEO gave the lowest antibacterial activity against both bacteria. This result led to the synergistic effect of the quaternization of GTMAC (40.7%) or methylation (36.1%) combined with the protonation on the CS backbone.

#### Bacteria Morphology After Contact with the Three Antibacterial Mats

Depending on the sophistication of the cell wall structure of the two types of bacteria, Figure 7 shows morphology of both bacteria contact on the three antibacterial mats. *S. aureus*, with a loose cell wall, had an average diameter of 0.8 μm on its spherical shape [Figure 7(a)] after the cells were fixed on the mat; they displayed an intact and normal surface appearance which implied that they are still alive. After the contact, they became deformed on HTACC and QBzCS fibrous mats. Some of the spheres were broken with opened surfaces. The *E. coli* bacteria, having a cylindrical shape with a longitude length of 1.5 μm as shown in Figure 7(b), have an outer membrane structure in the cell wall forming an additional barrier against foreign molecules to enter. After the contact, the cylindrical shape was elongated and distorted [shown with the arrows in Figure 7(c–f)]. The

cells were flattened and opened at one end or the other side of the tube. This indicated that some cell walls were damaged which may imply the release of intracellular components and obvious ruptures or pores on the cell surfaces.<sup>3,8</sup> All the treated bacteria had extra- and intracellular changes compared with the controls at zero time of contact. Therefore, upon the long contact time, both bacteria could be killed by QBzCS, HTACC, and CS/PEO fibrous mats.

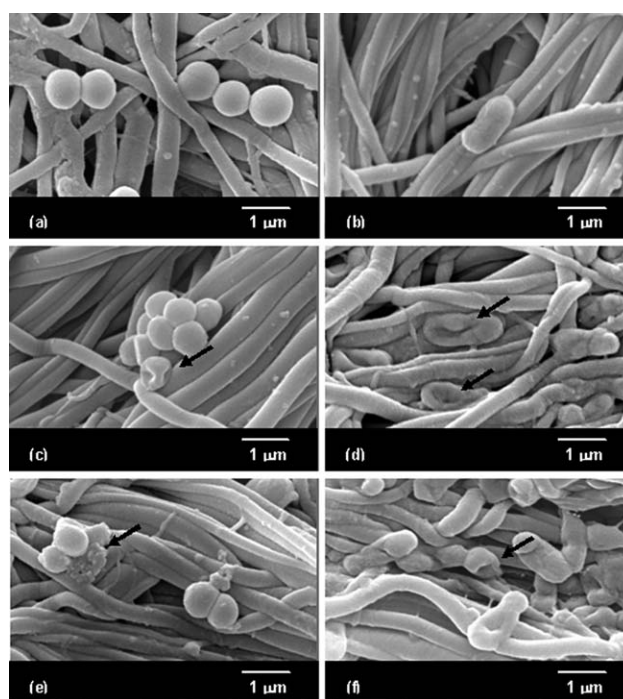


**Figure 7.** Morphologies of (a) *S. aureus* and (b) *E. coli* on the CS/PEO at initial time ( $t = 0$ ), (c) *S. aureus* on HTACC fibrous mat, (d) *E. coli* on HTACC fibrous mat, (e) *S. aureus* on QBzCS fiber mat, and (f) *E. coli* on QBzCS fibrous mat after 24 h contact.



Our observations are in good agreement with the statements of Kenawy et al.<sup>26</sup> and Helander et al.<sup>6</sup> who concluded that the antimicrobial activity of the polymers depends on adsorption and binding onto the bacterial cell surface, diffusion through the cell wall, and permeability through the cytoplasmic membrane, then disruption of the cytoplasmic membrane, leakage of the cytoplasmic constituents as shown by the black arrows, and death of the bacterial cells.

## CONCLUSIONS

Electrospun chitosan nanofibrous mats by blending chitosan with PEO in trifluoroacetic acid and dichloromethane mixed solvent were prepared. CS/PEO and the modified HTACC and QBzCS nanofibrous mats were successfully prepared, identified, and characterized by IR spectroscopy, XPS, and water swelling. *S. aureus* and *E. coli* tested with the three chitosan nanofibrous mats could reduce bacterial activities inevitably during 0.5–2 h of contact. The decreasing order of antibacterial activity was QBzCS > HTACC > CS/PEO. All the mats could better inhibit *S. aureus* than the *E. coli*. Both bacteria were killed through surface sloughing, breaching and pore openings on the surface. It was found that antibacterial efficiencies, against *S. aureus* or *E. coli*, of the two modified spun mats at the earlier stage of contact, such as 1 h, are beneficial for medical care.

## ACKNOWLEDGMENTS

The authors gratefully thank the Thailand Research Fund and the Commission of Higher Education, Ministry of Education for funding the research under the Senior Scholarly Consolidation Grant no. RTA5080004 to SK. Many thanks go to the Department of Imaging and Printing Technology, the Petroleum and Petrochemical College, and National Nanotechnology Center, NSTDA for providing research facilities.

## REFERENCES

1. Begin, A.; Calsteren, V. M. R. *Int. J. Biol. Macromol.* **1999**, *26*, 63.
2. Khan, T. A.; Peh, K. K.; Ch'ng, H. S. *J. Pharm. Pharm. Sci.* **2000**, *2*, 303.
3. Muzzarelli, R.; Tarsi, R.; Filippini, O.; Giovanetti, E.; Biagini, G.; Varaldo, P. E. *Antimicrob. Agents Chemoth.* **1990**, *34*, 2019.
4. Papineau, A. M.; Hoover, D. G.; Knorr, D.; Farkas, D. F. *Food Biotechnol.* **1991**, *5*, 45.
5. Sudarshan, N. R.; Hoover, D. G.; Knorr, D. *Food Biotechnol.* **1992**, *6*, 257.
6. Helander, I. M.; Nurmiaho-Lassila, E. L.; Ahvenainen, R.; Rhoades, J.; Roller, S. *Int. J. Food Microbiol.* **2001**, *71*, 235.
7. Tashiro, T. *Macromol. Mater. Eng.* **2001**, *28*, 63.
8. Tan, H.; Ma, R.; Lin, C. Liu, Z.; Tang, T. *Int. J. Mol. Sci.* **2013**, *14*, 1854.
9. Fong, H.; Chun, I.; Reneker, D. H. *Polymer* **1999**, *40*, 4585.
10. Deitzel, J. M.; Kleinmeyer, J. D.; Hirvonen, J. K.; Tan, N. C. B. *Polymer* **2001**, *42*, 8163.
11. Deitzel, J. M.; Kleinmeyer, J.; Harris, D.; Tan, N. C. B. *Polymer* **2001**, *42*, 261.
12. Zhang, C.; Yuan, X.; Wu, L. L.; Han, Y. S. *Eur. Polym. J.* **2005**, *41*, 423.
13. Doshi, J.; Reneker, D. H. *J. Electrostat.* **1995**, *35*, 151.
14. Zeng, J.; Xu, X. Y.; Chen, X.; Liang, Q.; Bian, X.; Yang, L.; Jing, L. *J. Controlled Release* **2003**, *92*, 227.
15. Ohkawa, K.; Cha, D.; Kim, H.; Nishida, A.; Yamamoto, H. *Macromol. Rapid Commun.* **2004**, *25*, 1600.
16. Sangsanoh, P.; Supaphol, P. *Biomacromolecules* **2006**, *7*, 2710.
17. Seong, H. S.; Whang, H. S.; Ko, S. W. *J. Appl. Polym. Sci.* **2000**, *76*, 2009.
18. Kim, C. H.; Choi, J. W.; Jae, C. H.; Suk, C. K. *Polym. Bull.* **1997**, *38*, 387.
19. Vallapa, N.; Wiarachai, O.; Thongchul, N.; Pan, J.; Tangpasuthadol, V.; Kiatkamjornwong, S.; Hoven, V. P. *Carbohydr. Polym.* **2011**, *83*, 868.
20. Wiarachai, O.; Thongchul, N.; Kiatkamjornwong, S.; Hoven, V. P. *Colloids Surf. B: Biointerfaces* **2012**, *92*, 121.
21. Pakravan, M.; Heuzey, M.-C.; Ajji, A. *Polymer* **2011**, *52*, 4813.
22. Hasegawa, M.; Isogai, A.; Onabe, F.; Usuda, M. *J. Appl. Polym. Sci.* **1992**, *45*, 1857.
23. Tual, C.; Espuche, E.; Escoubes, M.; Domard, A. *J. Polym. Sci. Part B: Polym. Phys.* **2000**, *38*, 1521..
24. Schiffman, J. D.; Schauer, C. I. *Polym. Rev.* **2008**, *48*, 317.
25. Zhang, X.; Bai, R. *J. Colloid Interface Sci.* **2003**, *264*, 30.
26. Kenawy, E.-R.; Worley, S. D.; Broughton, S. D. R. *Biomacromolecules* **2007**, *82*, 1359.